

# Experimental Study of Zonal Flow, Geodesic Acoustic Mode and Turbulence Regulation in Edge Plasmas of the HL-2A Tokamak

K. J. Zhao 1), J. Q. Dong 1,2), L. W. Yan 1), W. Y. Hong 1), A. Fujisawa 3), Q. Li 1), J. Qian 1), J. Cheng 1), T. Lan 4), A. D. Liu 4), H. L. Zhao 4), D. F. Kong 4), Y. Huang 1), Yi Liu 1), X. M. Song 1), Q. W. Yang 1), X. T. Ding 1), X. R. Duan 1) and Yong Liu 1)

1) Southwestern Institute of physics, P. O. Box 432, Chengdu, China

2) Institute for Fusion Theory and Simulation, Zhejiang University, Hangzhou, China

3) National Institute for Fusion Science, Oroshi-cho, Toki 509-5292, Japan

4) Department of Modern Physics, University of Science and Technology of China, Hefei, China

E-mail contact main author: kjzhao@swip.ac.cn

**Abstract.** The coexistence of intensive low frequency zonal flows (LFZFs) and geodesic acoustic modes (GAMs) has been observed by identifying the spatial characteristics, i.e. the symmetries in poloidal and toroidal directions, and the finite radial wave number, using three-dimensional Langmuir probe arrays in the edge plasmas of HL-2A tokamak. The analysis of three wave coupling with ambient turbulence suggests that the zonal flows are possibly created by three wave coupling mechanism. The radial distribution of LFZF and GAM power clearly shows the transition from GAM dominant to GAM and low frequency zonal flow coexisting structures, moving from LCFS inwards, in ECRH and Ohmic plasmas. The intensity of LFZF and GAM increases with ECRH power. The energy partition among LFZF, GAM, and turbulence indicates that the GAM dominantly regulates turbulence near the LCFS, while both GAM and LFZF modulate turbulence in the inner region of the plasmas. The envelope modulation analyses show that the turbulence envelopes are well correlated and out of phase with the LFZFs and GAMs.

## 1. Introduction

Zonal flows (ZFs) are universal in turbulent systems such as magnetically confined laboratory and space plasmas as well as atmospheres of stars. The extensive studies in this field are aimed at understanding nonlinear processes responsible for the coherent structure formation and for anomalous cross-field transport induced by turbulent fluctuations.

It is widely accepted in recent years that the turbulence and the induced transport may be reduced or even suppressed by  $\vec{E} \times \vec{B}$  sheared flows, such as mean flows and ZFs [1-3]. The ZFs are induced by  $(m = 0, n = 0)$  radial electric field fluctuations with finite radial scales, generated by nonlinear interactions with ambient turbulences (ATs). Here,  $m/n$  is the poloidal/toroidal mode number of the fluctuations. Two kinds of ZFs have been observed in toroidal plasmas, i.e., near zero low frequency zonal flows (LFZFs) [3], and oscillatory geodesic acoustic modes (GAMs) [4].

The LFZFs and GAMs have been extensively investigated in recent years [5-11]. LFZFs and GAMs have been identified on DIII-D, Compact Helical System (CHS), HL-2A, respectively. The coexistence of LFZF and GAM has also been observed on HL-2A, but there, the GAM still dominates. The nonlinear coupling between LFZF and GAM with AT has been investigated with bicoherence analyses [8]. Besides, the interactions have been observed as the single frequency modulation in the envelope of ATs [8].

In this paper, the coexistence of intensive LFZFs and GAMs is unambiguously identified by verifying the toroidal and poloidal symmetries, and the radial scale of the LFZFs and GAMs, with three dimensionally displaced Langmuir probe arrays, simultaneously, in the edge plasmas of the HL-2A tokamak. The nonlinear three wave coupling between the zonal flows and turbulence, and the modulations in the envelopes of AT are also analyzed. The radial distributions of zonal flow power demonstrate the transition from GAM dominant to the coexistence of LFZFs and GAMs moving from plasma boundary inwards. Energy partition analyses further show that both GAM and LFZF regulate turbulence in inner region of plasmas.

## 2. Arrangements of the LP arrays

The spatio-temporal fluctuations of the floating electrostatic potential were measured with three Langmuir probe (LP) arrays distributed poloidally and toroidally (see Figure.1) in the experiment. A 10 tip rake probe array with 4 mm tip separation was set up poloidally orientated and named poloidal probe (PP). A second rake probe array of 12 tips was mounted in the radial direction and named radial probe (RP). A three step Langmuir probe (TSLP) array of 6 tips [5] and the second rake probe array form a fast reciprocating probe set of 18 tips and a 65 mm poloidal span, which was located in a poloidal cross section of 2100 mm away from the first rake probe array in the toroidal direction. The length and diameter of each tip are 3 and 2 mm. All of the probe sets were mounted at the outside middle plane of the tokamak up-down symmetrically. The PP and RP were used to measure the floating potential fluctuations while the TSLP array was for the measurements of the electron temperature and density in the experiment.

The major and minor radii of the HL-2A tokamak are  $R = 1.65\text{ m}$  and  $a = 0.4\text{ m}$ , respectively. The experiments presented here were conducted in Ohmic and ECR heating deuterium plasmas of a circular cross section. The parameters specially set for the experiments are the toroidal magnetic field  $B_t = 1.2\text{-}1.35\text{ T}$ , the plasma current  $I_p = 150\text{ kA}$ , the line average electron density  $\bar{N}_e \sim 1 \times 10^{19}\text{ m}^{-3}$ ,

edge electron temperature  $T_e \sim 50\text{-}80\text{ eV}$ , the boundary safety factor  $q_a = 3.5\text{-}4.0$ , the discharge duration  $t_d = 1.2\text{ s}$ . The collision frequency and the safety factor at the LP locations

are estimated as  $\nu_{ii} \sim 1\text{-}3 \times 10^8/\text{s}$  and  $q((r/a)=0.92) = 0.88 q_a$ . No significant signals were

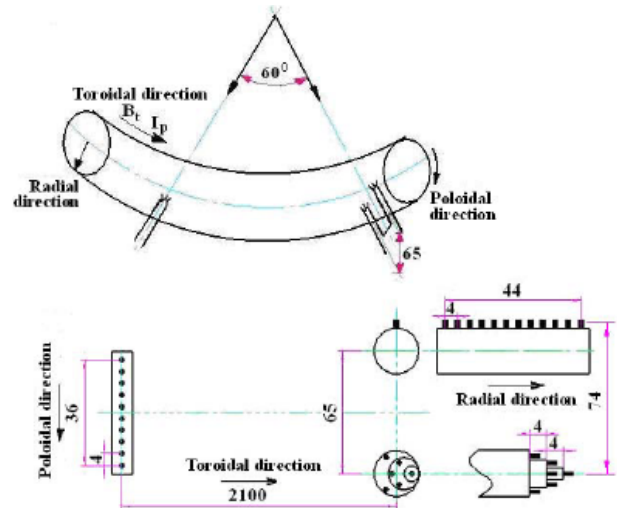


Figure 1. Layout and structure of the LP arrays.

detected when the LPs were placed outside the  $r=a$  surface.

The sampling rate of the probe data is 1 MHz corresponding to a Nyquist frequency of 500 kHz. The frequency resolution is 0.5 kHz in the following analysis unless otherwise stated.

### 3. The experimental results

#### 3.1. The coexistence of intensive LFZF and GAM

Figure 1 (a) presents the representative auto-power spectra of the floating potential fluctuations at the inner and outer radial positions whose locations are 28 mm and 24 mm inside the last

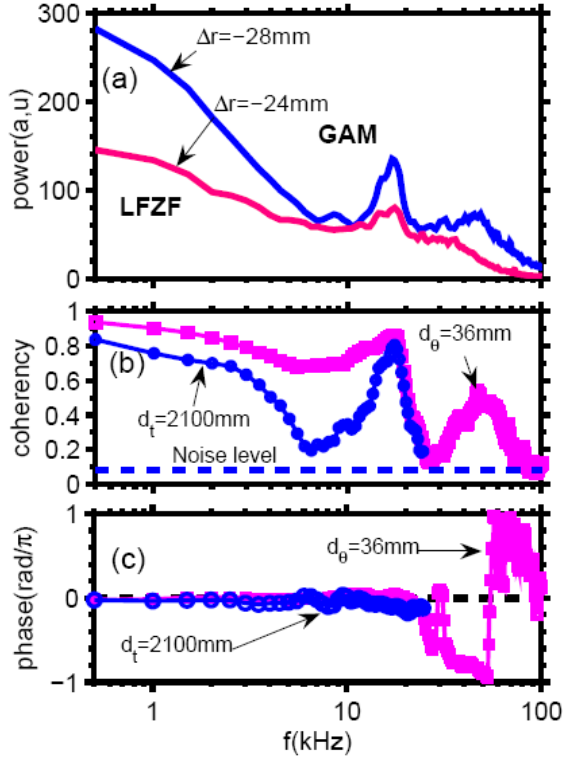


Figure.2. (a) Representative auto-power spectra of floating potentials at the inner and outer positions inside the last closed magnetic flux surface, (b) poloidal and toroidal coherency between floating potentials, (c) corresponding phase shifts.

$m=0.45\pm 0.07$  and  $n=0.33\pm 0.05$  were also estimated simultaneously for the GAM.

Besides, the two point correlation measurements of the potential fluctuations may provide wave number-frequency characteristics of the zonal flows. Shown in Figures 3(a) are the radial

wave number-frequency spectra,  $S(k_r, f)$ , where  $S(k, f) = \frac{1}{M} \sum_{i=1}^m I[k - k_i(f)] S_{crs,i}(f)$ ,

evaluated with two point correlation technique. Here,  $I(a-b)=1$  if  $a=b$ , otherwise,  $I(a-b)=0$ ,  $S_{crs,i}(f)$  and  $M$  represent the cross-correlation function and the number of realizations, respectively.

closed flux surface. Two distinct features are a large power fraction in low frequency range of 0-4kHz and a sharp peak at  $f \sim 17$  kHz. The former is the focus of this work and will be demonstrated as a LFZF while the latter was already identified as a GAM [5].

The similar features were observed in the coherency spectra of the floating potential fluctuations over 36 and 2100 mm poloidal and toroidal distances (the lines with squares and circles) as shown in Figure. 2(b). The corresponding cross phase spectra are given in Fig. 2(c). Quite high ( $\sim 0.8$ ) coherencies and near zero phase shifts are apparent in the frequency range of less than 4 kHz, besides in the GAM frequency vicinity. On average over the half width of the LFZF spectrum, the poloidal and toroidal mode numbers were estimated as  $m = 0.31 \pm 0.06$  and  $n = 0.020 \pm 0.004$ , respectively. This, in excellent agreement with theoretical and simulation predictions, unambiguously confirms the poloidal and toroidal symmetries of the fluctuations in this low frequency range in tokamak plasmas, as was done for the GAM alone before [5]. Here,

$S(k_r, f)$  and power density of LFZF and GAM as a functions of  $k_r$  are shown in figure 3 (b). The radial wave number and the half width of the  $S(k_r)$  spectrum are roughly estimated as  $k_r=0.5 \text{ cm}^{-1}$  and  $\Delta k_r = 3.7 \text{ cm}^{-1}$ , respectively, for the LFZF, in contrast with  $k_{rGAM} = 2.0 \text{ cm}^{-1}$  and  $\Delta k_{rGAM} = 4.0 \text{ cm}^{-1}$  for the GAM.

Figure 3(c) and (d) provide the coherence and phase shift of floating potentials at two positions with poloidal and radial spans of 74 mm and 4 mm. Quite high coherency up to  $\sim 0.7$  is shown again for the LFZFs and GAMs. In addition, there are significant phase shifts in the low frequency range of less than 4 kHz and GAM frequency range. The radial phase shifts seems to have approximately linear dispersion relations, which needs further investigation in future. The radial phase velocities of the LFZF and GAM are also estimated as 0.25 km/s and 0.33 km/s, respectively. The group velocity of the former is the same as the phase velocity while it is 0.27 km/s for the latter.

The spatial calibration accuracy for the LP radial positions is about 1 mm. That may induce a finite wave vector component in the direction connecting the two poloidal LPs as  $k \sim k_r/36 = 0.01 \text{ cm}^{-1}$  and  $m \sim 0.4$  from a finite radial wave vector  $k_r = 0.5 \text{ cm}^{-1}$  when the poloidal wave vector is zero. This may explain the deviation of the measured poloidal feature of the LFZFs from the  $m=0$  symmetry. Therefore, the observation, in excellent agreement with theoretical and simulation predictions, unambiguously confirms the poloidal and toroidal symmetries of the fluctuations of the LFZF in tokamak plasmas, as was done for the GAM alone before [5].

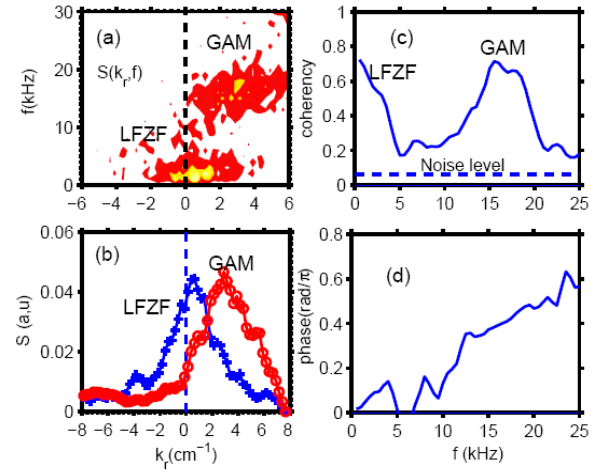


Figure3. (a)  $S(k_r, f)$  of potential fluctuations, (b) power density as a function of  $k_r$  for the LFZF and GAM, (c) and (d) coherencies and phase shifts between floating potential fluctuations with poloidal/radial spans of 74/ 4mm, respectively.

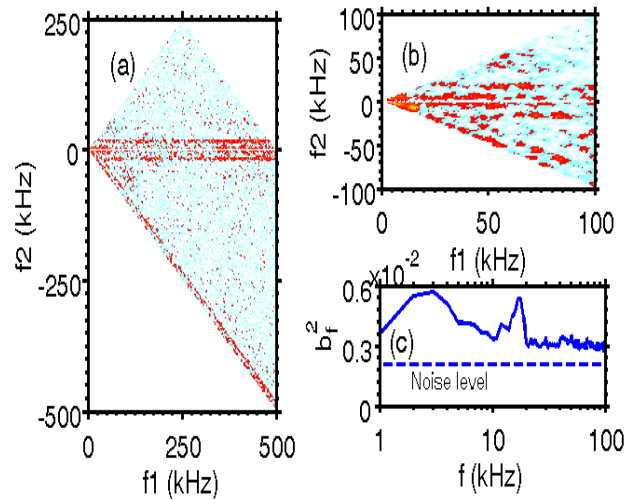


Figure4. (a) Auto-bicoherences of floating potentials plotted in  $f_1$ - $f_2$  plane and (b) corresponding to enlarge picture, (c) the total bicoherence.

### 3. 2. The nonlinear coupling between turbulence and zonal flows

The other condition for zonal flow to satisfy is the existence of the interaction with the AT or three wave coupling between ZF and AT. The bicoherence analysis, an indicator for the strength of nonlinear three wave coupling, can be used to prove the existence of the interaction between ZF and AT. The squared auto-bicoherence  $\hat{b}^2(f_3)$  of the perturbations is calculated and shown in Figure 4(a), plotted in the region between the lines of  $f_1=f_2$  and  $f_1=-f_2$  of the  $f_1$ -- $f_2$  plane. The enlarge picture in the frequency of less than 100kHz is also given in Figure 4 (b). The values of  $\hat{b}^2(f_3)$  about  $f_3=f_1-|f_2|<4\text{kHz}$  and  $f_2<4\text{kHz}$  as well as  $f_3=f_1-|f_2|\sim 17\text{kHz}$  and  $f_2\sim 17\text{kHz}$  are higher than the rest, indicating that the nonlinear three wave coupling is a plausible creating mechanism for the zonal flows. Figure 4.(c) provides the total bicoherence. Similar features as in the Figure 2(a) are clearly shown again. The frequency resolution is 1 kHz in this analysis and the signals are significantly above the noise level in the LFZF and GAM frequency ranges. Therefore, the fluctuations of less than 4 kHz and  $\sim 17$  kHz clearly demonstrate the coexistence of intensive low frequency zonal flow and GAM.

### 3. 3. Radial distributions of zonal flow power

Figure.5(a) shows radial distributions of the LFZF potential power in Ohmic (squares) and ECRH (cycles) plasmas. The same profiles for the GAM are also given in Figure 5 (b). Moving from the boundary inward, the intensity of LFZF first increases slightly, and then sharply rises up at the location of  $\sim 2.5$  cm where the GAM power reaches a minimum after a maximum at the position of  $\sim 1.5$  cm. The power of LFZF and GAM increases/decreases in radial direction more quickly in ECRH plasma than in Ohmic case. The radial profiles of the radial electric field fluctuations given in Figure. 5 (c) and (d) for the LFZF and GAM are similar to those of potentials. The radial distribution of low frequency zonal flow and GAM amplitudes clearly demonstrate a transition from GAM dominant to the coexistence structures, moving from boundary inwards. The processes may attribute to variations of the turbulence strengths and safety factor or collision damping. In addition, the intensity of LFZF and GAM increases with ECRH power, which is consistent with the mechanism of zonal flow generation by nonlinear interaction with turbulence as mentioned above. The radial profiles of LFZF and GAM powers do not vary significantly with ECRH power.

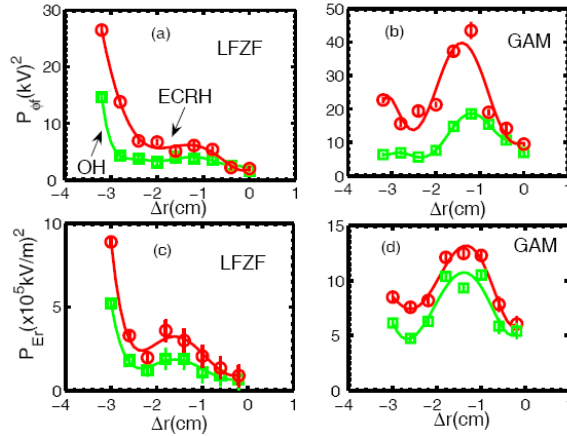


Figure.5 The power of potential fluctuations as a function of radial position for the LFZF (a) and GAM (b) in Ohmic and ECRH plasmas, respectively, and their radial electric field fluctuation power (c) and (d).

The energy partition among the LFZF, the GAM and the AT, depending on the local plasma parameters and influencing transport phenomena, is roughly estimated as a function of the radial position. Figure 6. (a)-(d) show the power fraction distributions of the LFZF, GAM, LFZF+GAM, and AT in Ohmic (the light lines) and ECRH (the heavy lines) plasmas, respectively. The LFZF power fraction increases toward inside, while the power fraction for the GAM sharply increases firstly, and gets a maximum, then rapidly decreases toward inside. The AT power fraction appears to have an anti-phase correlation with the total power partition of the LFZF and GAM inside the LCFS. The profiles of them are also similar in both OH and ECRH cases. This analysis suggests that the GAM predominantly suppresses the AT near the LCFS, while both LFZF and GAM have significant effects on the AT in inner plasma region. It seems that the LFZF and GAM fraction decreases with ECRH power, while that of AT increases. This may explain that the confinement degenerates in L-mode plasmas.

### 3. 4 Turbulence envelope modulations

The interaction between the ZFs and turbulence, especially the effect of the former on the latter, is a key issue in the study of transport in magnetized plasmas. The interaction can, in general, manifest as turbulence envelope (TE) modulation by ZFs. Figure 7 (a) shows the temporal evolutions of the LFZF and the TE in the frequency band of  $300 \text{ kHz} < f < 500 \text{ kHz}$ . One can see a clear out of phase correlation between them, (the signals of the TE are band-pass filtered for the LFZF frequency range  $0.3\text{-}4\text{kHz}$ ). Shown in Figure 7 (b) are the waveforms of the GAM and the TE. out of phase correlation between them is clearly shown again. Shown in Figure.7 (c) are the auto-power spectra of the TE at the radial positions of 2.4, 2.8 and 3.2 cm, respectively, inside the LCFS in Ohmic plasmas. The peaks at the LFZF and GAM frequencies are similar to those of potential fluctuations themselves. Therefore, it is obvious that zonal flows, including GAMs, should have significant impacts on the turbulence.

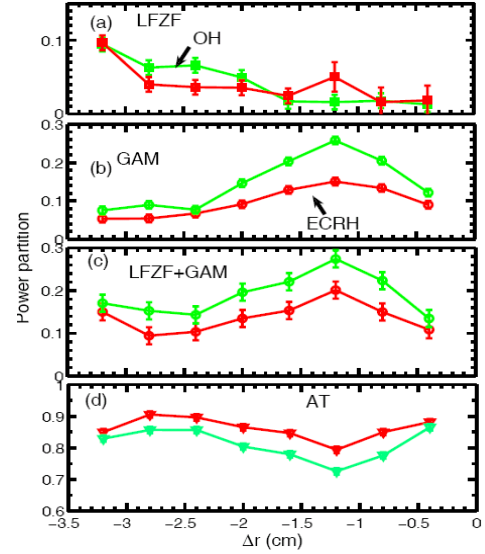


Figure. 6 The radial distributions power fraction of the LFZF (a), the GAM (b), the LFZF+GAM(c), and the AT (d) in Ohmic and ECRH plasmas.

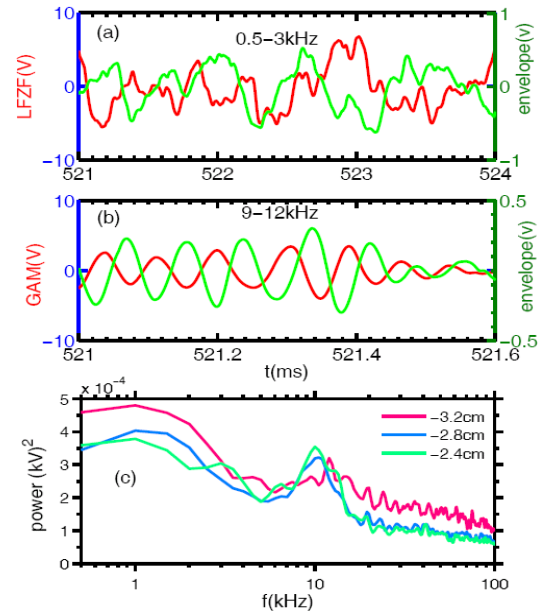


Figure.7 The waveforms of (a) LFZF and turbulence envelope and (b) GAM and turbulence envelope; (c) the power spectra of turbulence envelopes.

The spatial property of the TEs is investigated using the coherence between the potentials at two distant positions. Here, the selected frequency band of turbulence is from 300 to 500 kHz for evaluating the envelopes since the nonlinear coupling between ZFs and ATs in this frequency band range is stronger than that of the others. Figures 8 (a) and (b) show the coherences and phase shifts between the envelopes at two positions separated in the poloidal and toroidal directions. The significant coherence (higher than 0.2) and very low phase shift ( $m \approx 0.34 \pm 0.02$  and  $n \approx 0.1 \pm 0.1$ ) show the symmetric property of the turbulence envelope modulation. The two-point correlation technique is used to evaluate the radial scales of the TEs. As shown in Figure 8 (c), the radial wave number-frequency spectra for TE are very similar to that of the floating potentials themselves. As further confirmation, Figures 8 (d) and (e) provide a comparison of the radial wave-number spectra at the frequencies of the LFZF and GAM versus that of the TEs. The good agreement implies that the spatial characteristics of the TEs are identical to that of the LFZF and GAM. This result provides another strong evidence that the turbulence modulation effects are caused by the interaction between the zonal flows and the turbulence.

#### 4. Discussion

It is worth while to discuss the possible mechanisms of the turbulence modulation by the LFZFs and GAMs. One of the important origins, which should be distinguished from the ZF-AT interaction, is the Doppler effects due to the movements of the LFZFs and GAMs. If the fluctuation power is inhomogeneous with respect to the frequency in the plasma frame, the frequency modulation due to the Doppler effects in the laboratory frame should cause apparent modulation in the turbulence power of a frequency band. The power modulation due to the Doppler effects may be expressed in the simple form as  $\Delta P = (dP(f_0)/df)\delta f_{\max}$ , over the turbulence power spectra at the center of a band  $P(f_0)$ , where  $f_{\max} = k_{\theta}(f_0)v_{ZF,\max}$ . A rough estimate for the present experiment shows that the modulations are typically  $\sim 1\%$  and  $\sim 10\%$  due to the Doppler effects and the ZFs, respectively, for the frequency band from 350 to 400 kHz. Therefore, the nonlinear interactions between the ZFs and turbulence provide a possible explanation for the observed turbulence modulation.

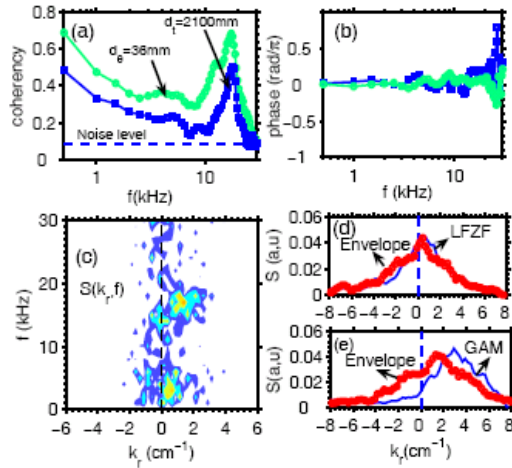


Fig. 8 (a) Poloidal and toroidal coherences between TEs (the light and dark lines) at the same two positions as those in Fig.2, (b) corresponding cross phases. (c) Radial wavenumber-frequency spectrum of the TE. (d) The radial wavenumber spectra of the floating potential and the TE for the LFZF, and (e) that for the GAM.

## 5. Conclusions

The coexistence of intensive LFZFs and GAMs has been observed by identifying the spatial characteristics, i.e. the symmetries in the poloidal and toroidal directions, and the finite radial wave number, in the edge plasma of HL-2A tokamak. The nonlinear couplings with ambient turbulence indicate that the zonal flows, including GAMs, are possibly created by the three wave coupling. The radial distributions of LFZF and GAM power clearly show the transition between the GAM dominant and GAM and LFZF coexistence structures, moving from the LCFS inwards in ECRH and Ohmic plasmas. The transition may attribute to variations of the turbulence strength and safety factor or collision damping.. The intensities of LFZF and GAM increase with ECRH power, in consistence with the model for the mechanism of zonal flow generation by nonlinear interaction with turbulence. The energy partition among the LFZF, the GAM and the AT, suggests that the GAM predominantly suppresses the AT near the LCFS, while both the GAM and LFZF have significant effects on the AT in inner region of plasmas. Furthermore, the spatial structures of on the turbulence envelopes in the frequency regimes of LFZF and GAM are similar to those observed in LFZFs and GAMs. These analyses clearly demonstrate that the zonal flows including GAMs, indeed have significant impacts on the turbulence in the edge plasmas of a tokamak.

## Acknowledgments

This work was partly supported by the National Natural Science Foundation of China Grants No.10775044, the Sichuan Youth Foundation of Science and Technology, Grant No 09ZQ026-079, and the National Magnetic Confinement Fusion Science Program Grant No 2010GB106008, this work was also supported by the JSPS-CAS Core-University Program in the field of ‘Plasma and Nuclear Fusion’.

## Reference

- [1] Lin Z et al 1998 Science **281**, 1835.
- [2] Diamond P H et al 2005 Plasma Phys. Controlled Fusion **47**, R35.
- [3] Hasegawa A and Wakatani M 1987 Phys. Rev. Lett. **59**, 1581.
- [4] Winsor N, Johnson J L, and Dawson J M 1968 Phys. Fluids **11**, 2448.
- [5] Zhao K J et al 2006 Phys. Rev. Lett. **96**, 255004.
- [6] Zhao K J et al 2007 Phys. plasmas **14**, 122301.
- [7] Lan T et al 2008 Plasma Phys. Controlled Fusion **50**, 045002.
- [8] Fujisawa A, 2009 Nucl. Fusion **49**, 013001.
- [9] Fujisawa A et al 2004 Phys. Rev. Lett. **93**, 165002.
- [10] Liu A D et al 2009 Phys. Rev. Lett. **103**, 095002.
- [11] Gupta D K et al 2006 Phys. Rev. Lett. **97**, 125002.